Nanochem Res 4(2): 154-162, Summer and Autumn 2019

RESEARCH PAPER

Co_3O_4/NiO@GQDs@SO_3H nanocomposite as an effective catalyst for the synthesis of pyranopyridines

Hossein Shahbazi-Alavi [1*], Ali Kareem Abbas [2], Javad Safaei-Ghomi [3]

[1] Young Researchers and Elite Club, Kashan Branch, Islamic Azad University, Kashan, Iran, Iran

[2] College of applied medical sciences, University of Kerbala, Iraq

[3] Department of Organic Chemistry, Faculty of Chemistry, University of Kashan, Kashan, Iran

ARTICLE INFO

Article History:
Received 26 June 2019
Accepted 17 September 2019
Published 15 October 2019

Keywords:
Nanocomposite
One-pot
Heterogeneous catalysts
Pyranopyridines
Nanoanalysis

ABSTRACT

Co_3O_4/NiO@GQDs@SO_3H nanocatalyst has been used as an effective catalyst for the preparation of benzopyranopyridines through a four-component reaction of salicylaldehydes, thiols and 2 equiv of malononitrile under reflux condition in ethanol. The catalyst has been characterized by FT-IR, XRD, SEM, EDS, BET, XPS, TGA and VSM. Atom economy, reusable catalyst, low catalyst loading and high yields of products are some of the notable features of this method. The best results were gained in EtOH and we found the convincing results for the reaction in the presence of Co_3O_4/NiO@GQDs@SO_3H nanocomposite (4 mg) under reflux conditions. Also, a series of salicylaldehydes and different thiols were studied under optimum conditions.

How to cite this article
Shahbazi-Alavi H, Kareem Abbas A, Safaei-Ghomi J. Co_3O_4/NiO@GQDs@SO_3H nanocomposite as an effective catalyst for the synthesis of pyranopyridines. Nanochem Res, 2019; 4(2):154-162. DOI: 10.22036/ncr.2019.02.007

INTRODUCTION

Pyranopyridines show biological activities including antipsychotic [1], anti-inflammatory [2], anti-asthma [3], antiallergic [4] and antibacterial [5]. These activities make benzopyranopyridines attractive targets in organic synthesis. A number of procedures have been developed for the preparation of pyranopyridines using K_2CO_3 [6], Et_3N [7,8] and NaOH [9]. Despite the use of these ways, there remains a need for further new methods for the synthesis of benzopyranopyridines. GQDs have achieved intense attention owing to the remarkable features containing biological [10], biomedical [11], drug delivery [12], photocatalysts [13], surfactants [14], electrochemical biosensing [15], electrocatalytic [16], Li-ion battery [17], optical properties and photovoltaic applications [18], photoluminescence [19-20], bioimaging properties [21], and catalytic activity [22]. Potential applications of N-graphene quantum dots were lately reviewed on the basis of theoretical and experimental studies [23-26]. Preparation of the highly efficient nanocomposite catalysts for the synthesis of organic compounds is still an attractive challenge. To attain larger surface area, nanocatalysts are functionalized by active groups [27-29]. The decoration of the nanoparticles with GQDs prevents the aggregation of fine particles and thus increases the efficient surface area and the number of reactive sites for an effective catalytic reaction. The -SO_3H and -COOH groups can be used as acid catalysts for many reactions [22-30]. Herein, we reported the use of Co_3O_4/NiO@GQDs@SO_3H nanocomposite as an efficient catalyst for the preparation of benzopyranopyridines through a four-component reaction of salicylaldehydes, thiols and 2 equiv of malononitrile under reflux condition in ethanol (Scheme 1).

EXPERIMENT

Materials and characterization

The powder X-ray diffraction was taken on a Philips diffractometer of X'pert Company with monochromatized Cu Kα radiation (λ = 1.5406

* Corresponding Author Email: *hossien_shahbazi@yahoo.com*

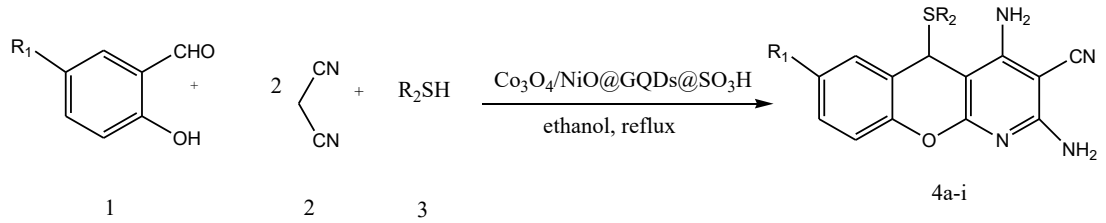

Scheme 1. The preparation of benzopyranopyridines using Co_3O_4/NiO@GQDs@SO_3H nanocatalyst

Å). The X-ray photoelectron spectroscopy (XPS) spectra were determined on an ESCA-3000 electron spectrometer. The microscopic morphology of nanocatalyst was performed by SEM (MIRA3). The thermogravimetric analysis (TGA) curves are gained by V5.1A DUPONT 2000. The magnetic measurement of samples was registered in a vibrating sample magnetometer (VSM) (Iran, Kashan Kavir). Surface area was carried out using nitrogen adsorption measurement (Micrometrics ASAP-2000).

Preparation of Co_3O_4/NiO nanoparticles

$NiCl_2$ and $Co(NO_3)_3$ with 1:3 molar ratio were dissolved in ethylene glycol. The appropriate amount of aqueous ammonia solution (28 wt%) was added to the above solution until the pH value reached 10. The transparent solution was placed in autoclave at 150 °C for 4h. The obtained precipitate was washed twice with CH_3OH and dry at 60 °C for 8h. Finally, the product was calcined at 500 °C for 2h.

Preparation of Co_3O_4/NiO@N-GQDs nanocomposite

1 g citric acid was dissolved into 20 mL deionized water, and stirred to form a clear solution. 0.3 mL ethylenediamine was added to the above solution and mixed to gain a clear solution. Then, 0.1 g of Co_3O_4/NiO nanoparticles was added to the mixture. The mixture was stirred at room temperature within 5 minutes. Then, the solution was transferred into a 50 ml Teflon lined stainless autoclave. The sealed autoclave was heated to 180°C for 12 hours in an electric oven. Finally, as-prepared nanostructured Co_3O_4/NiO@GQDs was obtained, washed several times with deionized water and ethanol, and then dried in an oven until constant weight was obtained.

Preparation of Co_3O_4/NiO@GQDs@SO_3H nanocomposite

1000 mg of Co_3O_4/NiO@N-GQDs nanocomposite was dispersed in dry CH_2Cl_2 (10 mL) and sonicated for 5 min. Afterward, chlorosulfonic acid (0.8 mL in dry CH_2Cl_2) was added drop-wise to a cooled (ice-bath) mixture of Co_3O_4/NiO@N-GQDs, during 30 min under N_2 with vigorous stirring. The mixture was stirred for 2 h, while the residual HCl was removed by suction. The resulted Co_3O_4/NiO@GQDs@SO_3H nanocomposite was separated, washed several times with dried CH_2Cl_2 before being dried under vacuum at 60 °C.

General procedure for the synthesis of benzopyranopyridines

A mixture of salicylaldehyde (1.5 mmol), malononitrile (3 mmol), a desired thiol (1.5 mmol), and Co_3O_4/NiO@GQDs@SO_3H nanocatalyst (4 mg) were stirred in 5 mL ethanol under reflux condition. The reaction was monitored by TLC. The formed precipitate was isolated by filtration. The product was dissolved in DMF (8 mL) and the catalyst was filtered. Then, water (5 mL) was added to the filtrate which resulted in the crystallization of the product. The resulting crystalline structure was filtered and dried with a vacuum pump. Spectra data 4a and 4c compounds are presented:

2,4-Diamino-5-(phenylthio)-5H-[1]benzopyrano[2,3-b]pyridine-3-carbonitrile **4a**: yellow solid, m.p. 220–222 °C. IR (KBr): ν = 3425, 3354 (NH_2), 2200 (C≡N), 1625 (C=N), 1574, 1414 (C=C), 695 (C-S-C) cm^{-1}. ^1H NMR (400 MHz, DMSO-d_6): δ (ppm) = 5.71 (s, 1H, H-5), 6.52-6.72 (2H, m), 6.70-6.74 (3H, m), 6.95 (s, 2H, NH_2), 7.06-7.14 (4H, m, NH_2 and ArH), 7.16-7.35 (m, 2H,). ^{13}C NMR (100 MHz, DMSO-d_6): δ (ppm) = 43.2, 70.7, 86.8, 116.3, 116.7, 121.4, 123.4, 128.7, 128.8, 129.6, 129.9, 134.3, 137.5, 150.8, 156.5, 159.8, 160.8. – Analysis for $C_{19}H_{14}N_4OS$: calcd. C 65.88, H 4.07, N 16.17, S 9.26. Found C 65.80, H 4.18, N 16.02, S 9.18.

2,4-Diamino-5-[(phenylmethyl)thio]-5H-[1]benzopyrano[2,3-b]pyridine-3-carbonitrile **4c**: yellow solid, mp 175–177 °C. IR (KBr): ν = 3375, 3437 (NH_2), 2202 (C≡N), 1625 (C=N), 1542 and 1484 (C=C), 702 (C-S-C) cm^{-1}. ^1H NMR (400 MHz, DMSO-d_6): δ (ppm) = 3.52 (ABq, 2H, J = 12Hz,

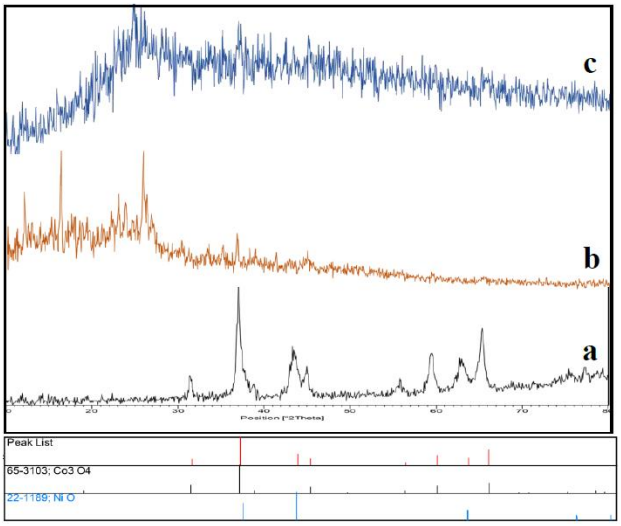

Fig. 1. XRD pattern of (a) Co_3O_4/NiO, (b) Co_3O_4/NiO@GQDs and (c) Co_3O_4/NiO@GQDs @ SO_3H

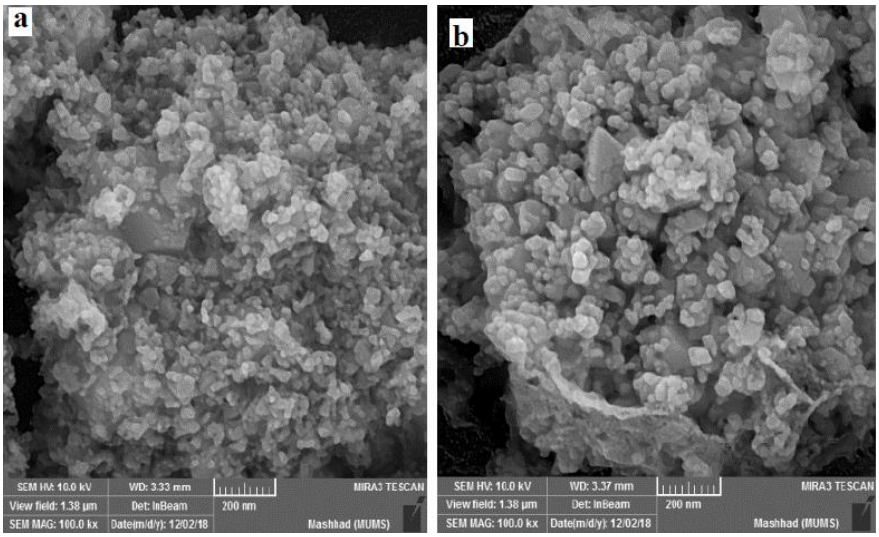

Fig. 2. SEM images of (a) Co_3O_4/NiO, and (b) Co_3O_4/NiO@GQDs @SO_3H

CH_2), 5.40 (s, 1H), 6.56 (bs, 2H, NH_2), 6.84 (bs, 2H, NH_2), 7.04–7.25 (m, 7H, ArH), 7.35 (m, 2H, ArH). ^{13}C NMR (100 MHz, DMSO-d_6): δ (ppm) = 35.1, 44.2, 70.8, 87.2, 117.5, 118.4, 119.2, 122.7, 124.3, 124.5, 129.7, 133.4, 133.4, 136.5, 143.8, 152.8, 159.5, 160.4; Analysis for $C_{20}H_{16}N_4OS$: calcd. C 66.65, H 4.47, N 15.54, S 8.90. Found C 66.48, H 4.52, N 15.42, S 8.82.

RESULTS AND DISCUSSION

In the beginning, we prepared Co_3O_4/NiO nanoparticles by easy techniques. A hydrothermal method was utilized for the preparation of N-GQDs [31]. Sulfonated graphene quantum dots were prepared using chlorosulfonic acid [32]. The XRD patterns of Co_3O_4/NiO, Co_3O_4/NiO@N-GQDs and Co_3O_4/NiO@GQDs @ SO_3H nanocomposite are indicated in Fig. 1. The XRD pattern confirms the presence of both NiO (JCPDS No.22-1189) and Co_3O_4 (JCPDS No 65-3103).

The SEM images of Co_3O_4/NiO and Co_3O_4/NiO@ GQDs@SO_3H nanocomposite are indicated in Fig. 2. The SEM images of the Co_3O_4/NiO@ GQDs@SO_3H nanocomposite showed the formation of uniform particles, and the energy-dispersive X-ray spectrum (EDS) confirmed the presence of Co, Ni, O, S and C species in the structure of the nanocomposite (Fig. 3).

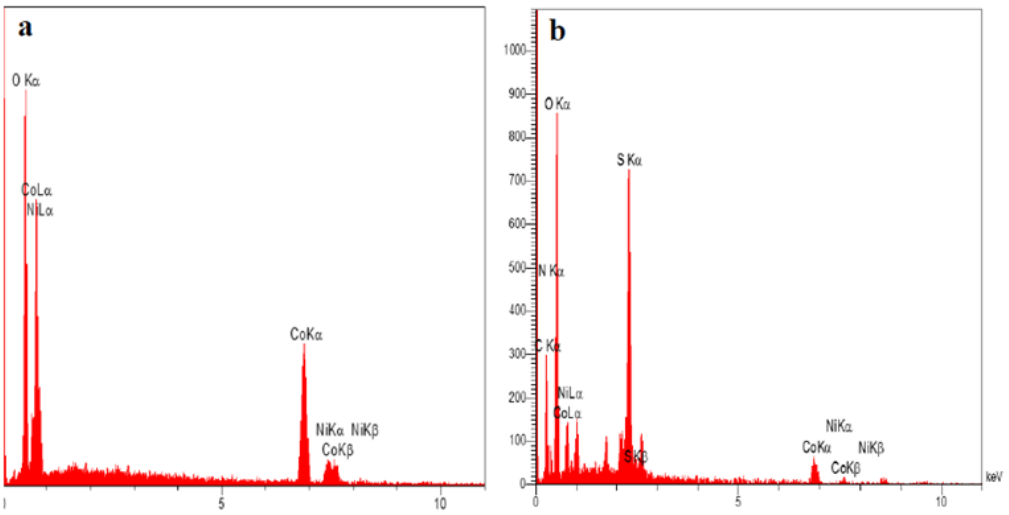

Fig. 3. EDS spectrum of (a) Co_3O_4/NiO, and (b) Co_3O_4/NiO@GQDs @SO_3H

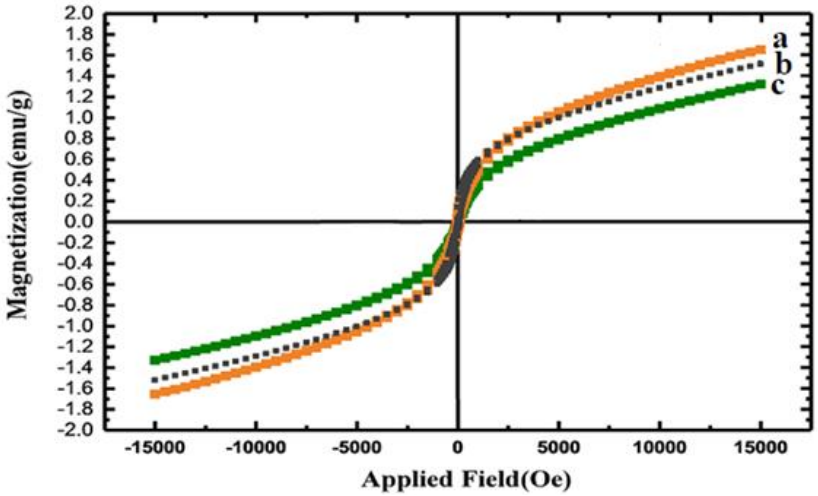

Fig. 4. VSM of (a) Co_3O_4/NiO, (b) Co_3O_4/NiO@GQDs and (c) Co_3O_4/NiO@GQDs @SO_3H

Magnetic properties of nanocomposites before and after their being decorated with GQDs were tested by vibrating-sample magnetometer (VSM) (Fig 4). The lower magnetism of the as-synthesized Co_3O_4/NiO@GQDs@SO_3H compared with the Co_3O_4/NiO was ascribed to the antiferromagnetic behavior of GQDs as a dopant. These results display that the magnetization properties decrease by coating and functionalization [33-34].

The FT-IR spectra of Co_3O_4/NiO, Co_3O_4/NiO@N-GQDs and Co_3O_4/NiO@GQDs @SO_3H nanocomposite are indicated in Fig. 5. The absorption peak at 3330 cm^{-1} related to the stretching vibrational absorptions of OH. The peaks at 461, 568, 657 cm^{-1} corresponded to the Ni-O, Co^{+2}-O and Co^{3+}-O, respectively. The characteristic peaks at 3442 cm^{-1} (O-H stretching vibration), 1706 cm^{-1} (C=O stretching vibration), 1126 cm^{-1} (C-O-C stretching vibration) appear in the spectrum of Fig. 5b. The peak at approximately 1474-1582 cm^{-1} is attributed to C=C bonds. The presence of sulfonyl group is also verified by the peaks appeared at 1214 and 1120 cm^{-1}. The broad peak at 3340 cm^{-1} is related to the stretching vibrational absorptions of OH (SO_3H) (Fig 5c).

The BET specific surface area of Co_3O_4/NiO and Co_3O_4/NiO@GQDs@SO_3H nanocomposites was determined by the nitrogen gas adsorption-desorption isotherms (Fig. 6). The results presented that the BET specific surface area of Co_3O_4/NiO

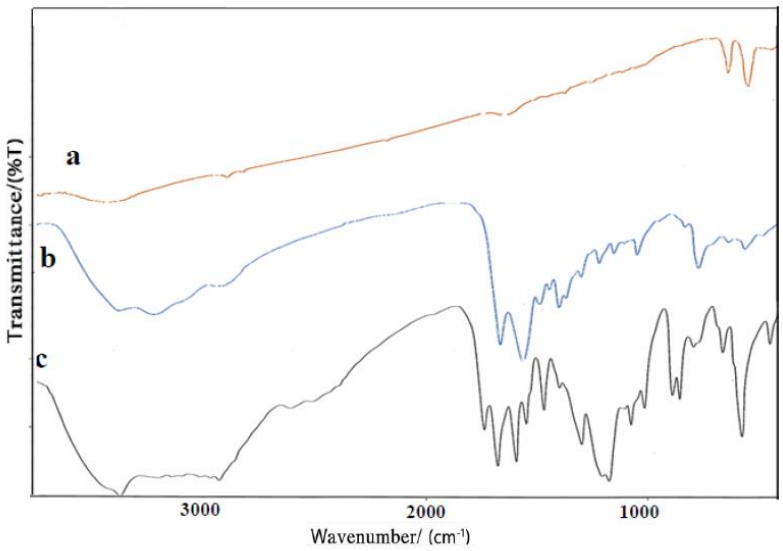

Fig. 5. FT-IR of (a) Co_3O_4/NiO, (b) Co_3O_4/NiO@GQDs and (c) Co_3O_4/NiO@GQDs @SO_3H

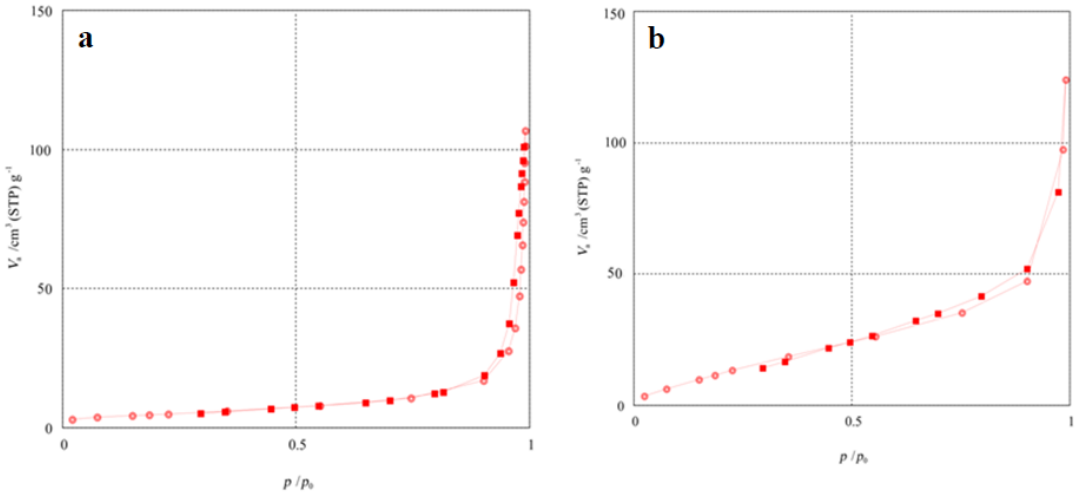

Fig. 6. The BET specific surface area of (a) Co_3O_4/NiO, and (b) Co_3O_4/NiO@GQDs @SO_3H

was improved from 12.24 to 32.44 m^2/g after modification with GQDs, therefore, more active sites were introduced on Co_3O_4/NiO@GQDs@SO_3H surface.

Thermogravimetric analysis determines the thermal stability of the Co_3O_4/NiO@GQDs@SO_3H nanocomposite (Fig. 7). The curve indicates a weight loss about 14.06 % from 150 to 500 °C which are attributed to the oxidation and degradation of GQD.

The X-ray photoelectron spectroscopy (XPS) analysis of Co_3O_4/NiO@GQDs@SO_3H nanocomposite is indicated in Fig. 8. In the wide-scan spectrum of nanocatalyst, the predominant components are Ni $2p_{3/2}$ (854.4 eV), Ni $2p_{1/2}$ (873.4 eV), Co $2p_{3/2}$ (780.4 eV), Co $2p_{1/2}$ (792.6 eV), O 1s (529.8 eV), N 1s (400 eV), C 1s (284.5 eV) and S 2p (164.3 eV).

Initially, we carried out four-component reaction of salicyladehyde (1.5 mmol), malononitrile (3.0 mmol) and benzenethiol (1.5 mmol) as a model reaction. The model reaction was performed by morpholine, *p*-TSA, $NaHSO_4NiO$, Co_3O_4, Co_3O_4/NiO, Co_3O_4/NiO@GQDs and Co_3O_4/NiO@GQDs@SO_3H nanocomposite. The best results were gained in EtOH and we received the

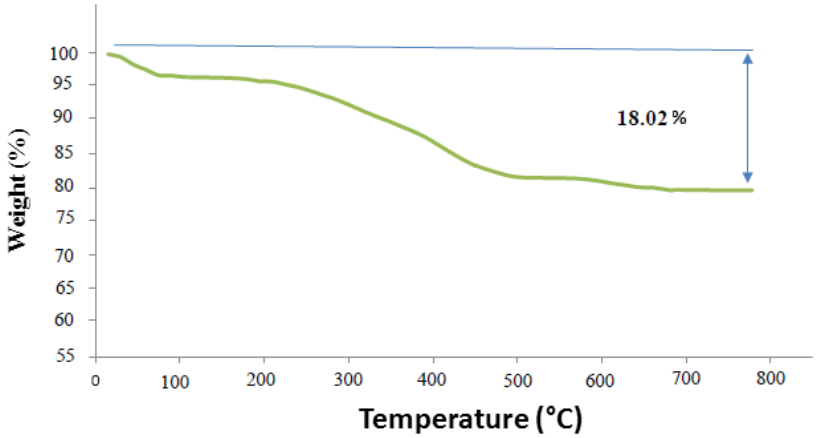

Fig. 7. TGA of Co_3O_4/NiO@GQDs @SO_3H nanocomposit

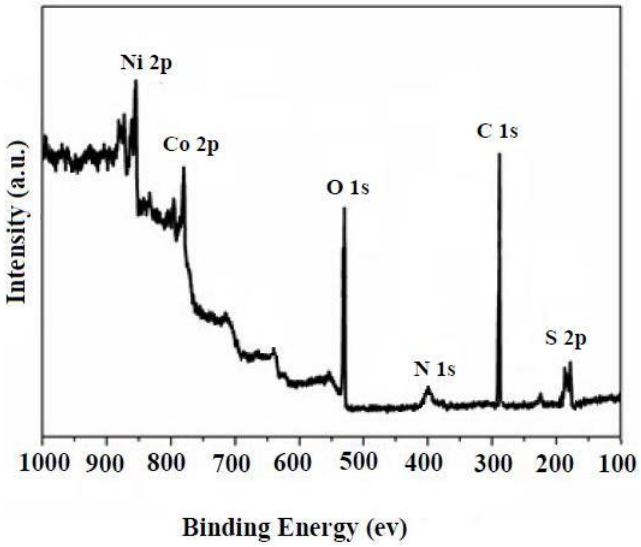

Fig. 8. X-ray photoelectron spectroscopy (XPS) analysis of nanocomposite

convincing results for the reaction in the presence of Co_3O_4/NiO@GQDs@SO_3H nanocomposite (4 mg) under reflux conditions (Tables 1). A series of salicylaldehydes and different thiols were studied under optimum conditions (Table 2). The results were good in yields.

We also determined recycling of Co_3O_4/NiO@GQDs@SO_3H nanocomposite as a catalyst for the model reaction under reflux conditions in ethanol. The results showed that nanocomposite can be reused several times without noticeable loss of catalytic activity (Yields 90 to 88%) (Fig. 9).

A plausible mechanism for the preparation of benzopyranopyridines using Co_3O_4/NiO@GQDs@SO_3H nanocomposites is indicated in Scheme 2. Firstly, salicylaldehyde reacts with 1 equiv of malononitrile to form intermediate $\mathbf{I}_1$ and subsequent intramolecular addition of the hydroxyl group to the C≡N gives the cyclic intermediate $\mathbf{I}_2$. This compound undergoes addition with thiophenol **3** to afford phenylsulfanylchromene $\mathbf{I}_3$. The intermediate $\mathbf{I}_3$ reacts with another equiv of malononitrile to form intermediate $\mathbf{I}_4$, followed by intramolecular cyclization to form intermediate $\mathbf{I}_5$. Finally the chromenopyridine **P** was formed by the tautomerization of the imino group to the amino group. The SO_3H groups distributed on the surface of Co_3O_4/NiO@GQDs activate the C=O, C=NH and C≡N groups for better reaction with nucleophiles.

Table 1. Optimization of reaction condition using different catalysts [a]

Entry	Catalyst (amount)	Solvent (reflux)	Time (min)	Yield %
1	none	EtOH	300	NR
2	morpholine (7 mol%)	EtOH	120	51
3	$NaHSO_4$ (4 mol%)	EtOH	250	42
4	ZrO_2 (4 mol%)	EtOH	150	42
5	*p*TSA (5 mol%)	EtOH	150	54
6	Nano-Co_3O_4	EtOH	150	49
7	Nano-NiO	EtOH	150	59
8	Co_3O_4/NiO nanocomposite	EtOH	150	65
9	Co_3O_4/NiO@GQDs nanocomposite	EtOH	150	76
10	Co_3O_4/NiO@GQDs@SO_3H nanocomposite (2 mg)	EtOH	25	82
11	Co_3O_4/NiO@GQDs@SO_3H nanocomposite (4 mg)	EtOH	25	90
12	Co_3O_4/NiO@GQDs@SO_3H nanocomposite (6 mg)	EtOH	25	90
13	Co_3O_4/NiO@GQDs@SO_3H nanocomposite (4 mg)	H_2O	50	65
14	Co_3O_4/NiO@GQDs@SO_3H nanocomposite (4 mg)	DMF	50	70
15	Co_3O_4/NiO@GQDs@SO_3H nanocomposite (4 mg)	CH_3CN	50	78

[a] Salicyladehyde (R_1 = H) (1.5 mmol), malononitrile (3.0 mmol), and benzenethiol (R_2 = C_6H_5) (1.5 mmol).
[b] Isolated yields

Table 2. Synthesis of benzopyranopyridines using Co_3O_4/NiO@GQDs@SO_3H nanocomposite (4 mg)

Entry	R_1 in aldehyde 1	R_2 in thiol 3	Product	Time (min)	Yield%[a]	m.p. found
1	H	C_6H_5-	**4a**	25	90	220-222
2	H	4-MeC_6H_4-	**4b**	35	85	223-225
3	H	$C_6H_5CH_2$-	**4c**	35	86	175-177
4	H	2-furanylmethyl-	**4d**	35	83	200-201
5	Br	C_6H_5-	**4e**	25	92	214-216
6	Br	4-MeC_6H_4-	**4f**	25	88	212-214
7	Br	$C_6H_5CH_2$-	**4g**	25	87	205-207
8	Br	2-furanylmethyl-	**4h**	30	83	223-225
9	Me	4-ClC_6H_4-	**4i**	40	82	280-282

[a] isolated yield

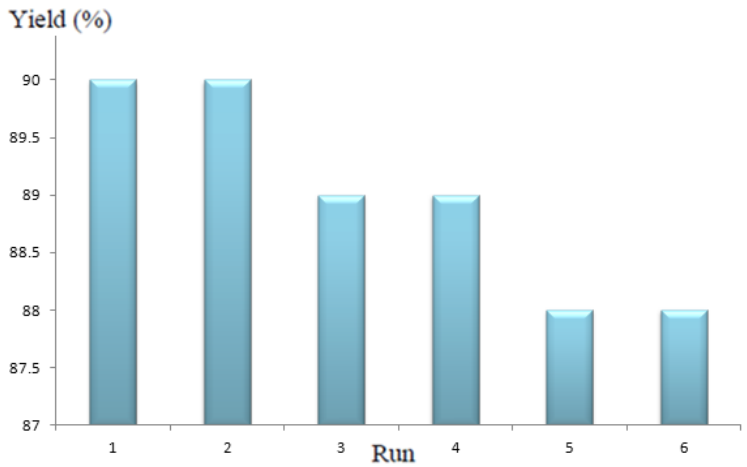

Fig. 9. Recycling of Co_3O_4/NiO@GQDs @SO_3H nanocomposite as a catalyst for the model reaction

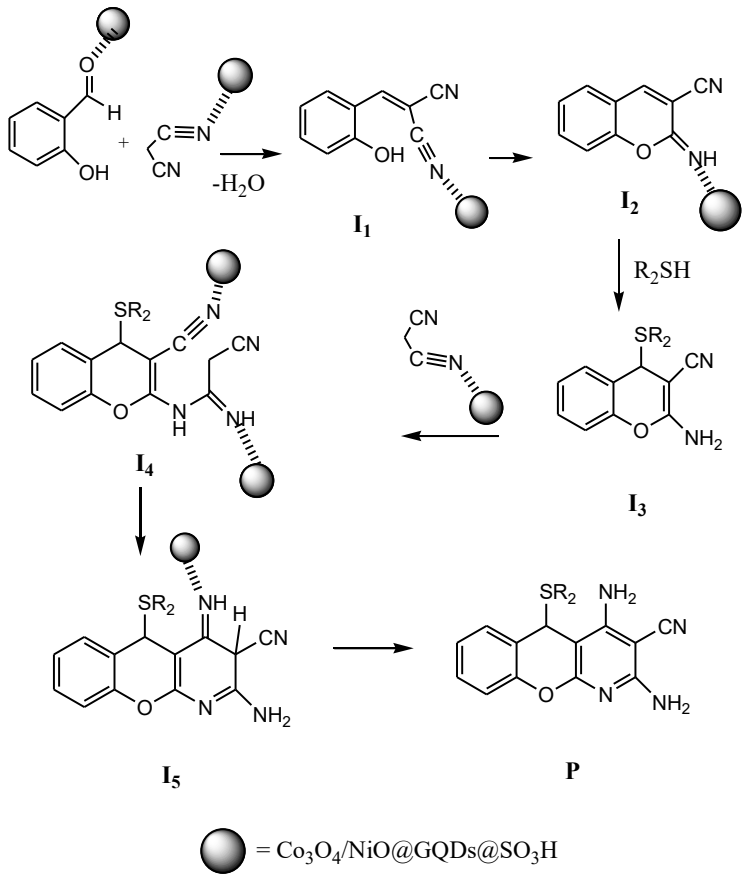

Scheme 2. Possible mechanism for the synthesis of benzopyranopyridines using Co_3O_4/NiO@GQDs@SO_3H nanocatalyst

CONCLUSION

In this study, we described the synthesis of benzopyranopyridines using Co_3O_4/NiO@GQDs@SO_3H nanocomposite as a superior catalyst under reflux conditions. The procedure offers several advantages including environmental friendliness, significantly shorter reaction time, reusability of the catalyst and low catalyst loading.

ACKNOWLEDGMENT

The authors are grateful to the University of Kashan for supporting this work under grant no. 159148/XII.

CONFLICT OF INTEREST

The authors declare that they have no conflict of interest.

REFERENCES

1. Unangst PC, Capiris T, Connor DT, Heffner TG, MacKenzie RG, Miller SR, et al. Chromeno[3,4-c]pyridin-5-ones: Selective Human Dopamine D4 Receptor Antagonists as Potential Antipsychotic Agents. Journal of Medicinal Chemistry. 1997;40(17):2688-93.
2. Hosni H, Abdulla M. Anti-inflammatory and analgesic activities of some newly synthesized pyridinedicarbonitrile and benzopyranopyridine derivatives. Acta Pharmaceutica2008. p. 175.
3. Ukawa K, Ishiguro T, Kuriki H, Nohara A. Synthesis of the metabolites and degradation products of 2-amino-7-isopropyl-5-oxo-5H-(1)benzopyrano(2,3-b)pyridine-3-carboxylic acid (Amoxanox). CHEMICAL & PHARMACEUTICAL BULLETIN. 1985;33(10):4432-7.
4. Goto K, Terasawa M, Maruyama Y. Anti-Allergic Activities of a New Benzopyranopyridine Derivative Y-12,141 in Rats. International Archives of Allergy and Immunology. 1979;59(1):13-9.
5. Frolova LV, Malik I, Uglinskii PY, Rogelj S, Kornienko A, Magedov IV. Multicomponent synthesis of 2,3-dihydrochromeno[4,3-d]pyrazolo[3,4-b]pyridine-1,6-diones: a novel heterocyclic scaffold with antibacterial activity. Tetrahedron Letters. 2011;52(49):6643-5.
6. Mishra S, Ghosh R. K2CO3-Mediated, One-Pot, Multicomponent Synthesis of Medicinally Potent Pyridine and Chromeno[2,3-b]pyridine Scaffolds. Synthetic Communications. 2012;42(15):2229-44.
7. Evdokimov NM, Kireev AS, Yakovenko AA, Antipin MY, Magedov IV, Kornienko A. Convenient one-step synthesis

of a medicinally relevant benzopyranopyridine system. Tetrahedron Letters. 2006;47(52):9309-12.
8. Evdokimov NM, Kireev AS, Yakovenko AA, Antipin MY, Magedov IV, Kornienko A. One-Step Synthesis of Heterocyclic Privileged Medicinal Scaffolds by a Multicomponent Reaction of Malononitrile with Aldehydes and Thiols. The Journal of Organic Chemistry. 2007;72(9):3443-53.
9. Osyanin VA, Osipov DV, Klimochkin YN. Convenient one-step synthesis of 4-unsubstituted 2-amino-4H-chromene-2-carbonitriles and 5-unsubstituted 5H-chromeno[2,3-b] pyridine-3-carbonitriles from quaternary ammonium salts. Tetrahedron. 2012;68(27-28):5612-8.
10. Zheng XT, Ananthanarayanan A, Luo KQ, Chen P. Glowing Graphene Quantum Dots and Carbon Dots: Properties, Syntheses, and Biological Applications. Small. 2014;11(14):1620-36.
11. Şenel B, Demir N, Büyükköroğlu G, Yıldız M. Graphene quantum dots: Synthesis, characterization, cell viability, genotoxicity for biomedical applications. Saudi Pharmaceutical Journal. 2019;27(6):846-58.
12. Molaei MJ. Carbon quantum dots and their biomedical and therapeutic applications: a review. RSC Advances. 2019;9(12):6460-81.
13. Yeh T-F, Teng C-Y, Chen S-J, Teng H. Nitrogen-Doped Graphene Oxide Quantum Dots as Photocatalysts for Overall Water-Splitting under Visible Light Illumination. Advanced Materials. 2014;26(20):3297-303.
14. Xi F, Zhao J, Shen C, He J, Chen J, Yan Y, et al. Amphiphilic graphene quantum dots as a new class of surfactants. Carbon. 2019;153:127-35.
15. Wang Y, Shao Y, Matson DW, Li J, Lin Y. Nitrogen-Doped Graphene and Its Application in Electrochemical Biosensing. ACS Nano. 2010;4(4):1790-8.
16. Li Q, Zhang S, Dai L, Li L-s. Nitrogen-Doped Colloidal Graphene Quantum Dots and Their Size-Dependent Electrocatalytic Activity for the Oxygen Reduction Reaction. Journal of the American Chemical Society. 2012;134(46):18932-5.
17. Reddy ALM, Srivastava A, Gowda SR, Gullapalli H, Dubey M, Ajayan PM. Synthesis Of Nitrogen-Doped Graphene Films For Lithium Battery Application. ACS Nano. 2010;4(11):6337-42.
18. Hasan MT, Gonzalez-Rodriguez R, Ryan C, Pota K, Green K, Coffer JL, et al. Nitrogen-doped graphene quantum dots: Optical properties modification and photovoltaic applications. Nano Research. 2019;12(5):1041-7.
19. Temerov F, Belyaev A, Ankudze B, Pakkanen TT. Preparation and photoluminescence properties of graphene quantum dots by decomposition of graphene-encapsulated metal nanoparticles derived from Kraft lignin and transition metal salts. Journal of Luminescence. 2019;206:403-11.
20. Zhu S, Song Y, Zhao X, Shao J, Zhang J, Yang B. The photoluminescence mechanism in carbon dots (graphene quantum dots, carbon nanodots, and polymer dots): current state and future perspective. Nano Research. 2015;8(2):355-81.
21. Qu D, Zheng M, Li J, Xie Z, Sun Z. Tailoring color emissions from N-doped graphene quantum dots for bioimaging applications. Light: Science & Applications. 2015;4(12):e364-e.
22. Sajjadi S, Khataee A, Darvishi Cheshmeh Soltani R, Hasanzadeh A. N, S co-doped graphene quantum dot–decorated Fe3O4 nanostructures: Preparation, characterization and catalytic activity. Journal of Physics and Chemistry of Solids. 2019;127:140-50.
23. Du Y, Guo S. Chemically doped fluorescent carbon and graphene quantum dots for bioimaging, sensor, catalytic and photoelectronic applications. Nanoscale. 2016;8(5):2532-43.
24. Yan Y, Gong J, Chen J, Zeng Z, Huang W, Pu K, et al. Recent Advances on Graphene Quantum Dots: From Chemistry and Physics to Applications. Advanced Materials. 2019;31(21):1808283.
25. Li M, Chen T, Gooding JJ, Liu J. Review of Carbon and Graphene Quantum Dots for Sensing. ACS Sensors. 2019;4(7):1732-48.
26. Wang Z, Zeng H, Sun L. Graphene quantum dots: versatile photoluminescence for energy, biomedical, and environmental applications. Journal of Materials Chemistry C. 2015;3(6):1157-65.
27. Hu E, Yu X-Y, Chen F, Wu Y, Hu Y, Lou XWD. Graphene Layers-Wrapped Fe/Fe5 C2 Nanoparticles Supported on N-doped Graphene Nanosheets for Highly Efficient Oxygen Reduction. Advanced Energy Materials. 2017;8(9):1702476.
28. Koli PB, Kapadnis KH, Deshpande UG, Patil MR. Fabrication and characterization of pure and modified Co3O4 nanocatalyst and their application for photocatalytic degradation of eosine blue dye: a comparative study. Journal of Nanostructure in Chemistry. 2018;8(4):453-63.
29. Hu E, Feng Y, Nai J, Zhao D, Hu Y, Lou XW. Construction of hierarchical Ni–Co–P hollow nanobricks with oriented nanosheets for efficient overall water splitting. Energy & Environmental Science. 2018;11(4):872-80.
30. Hu E, Ning J, He B, Li Z, Zheng C, Zhong Y, et al. Unusual formation of tetragonal microstructures from nitrogen-doped carbon nanocapsules with cobalt nanocores as a bi-functional oxygen electrocatalyst. Journal of Materials Chemistry A. 2017;5(5):2271-9.
31. Qu D, Zheng M, Du P, Zhou Y, Zhang L, Li D, et al. Highly luminescent S, N co-doped graphene quantum dots with broad visible absorption bands for visible light photocatalysts. Nanoscale. 2013;5(24):12272.
32. Qu D, Zheng M, Du P, Zhou Y, Zhang L, Li D, et al. Highly luminescent S, N co-doped graphene quantum dots with broad visible absorption bands for visible light photocatalysts. Nanoscale. 2013;5(24):12272.
33. Shahbazi-Alavi H, Safaei-Ghomi J. Nano-Fe_3O_4 attached to Crosslinked sulfonated polyacrylamide (Cross-PAA-SO_3H) as high performance catalyst for the synthesis of thiazoles under ultrasonic irradiations. Nanochemistry Research. 2019; 4(1): 55-63.
34. Shahbazi-Alavi H, Safaei-Ghomi J. Cross-linked sulfonated polyacrylamide (Cross-PAA-SO_3H) attached to nano-Fe_3O_4 as a superior catalyst for the synthesis of oxindoles. Journal of Nanoanalysis. 2019; 6(3): 185-92
35. Shahbazi-Alavi H, Safaei-Ghomi J. Cross-linked sulfonated polyacrylamide (Cross-PAA-SO3H) attached to nano-Fe3O4 as a superior catalyst for the synthesis of oxindoles. Journal of Nanoanalysis. 2019;6(3):185-92.